1st International Conference on Sensing Technology
November 21-23, 2005 Palmerston North, New Zealand

Structured Fiber Bragg Gratings for Sensing Applications

Agostino Iadicicco[a], Stefania Campopiano[a], Michele Giordano[b], Antonello Cutolo[a], Andrea Cusano[a]

[a] Optoelectronic Division- Engineering Department, University of Sannio, Corso Garibaldi, 107, 82100 Benevento, Italy; a.cusano@unisannio.it

[b] Institute of Composite Materials Technology National Research Council (ITMC-CNR)- Piazzale Enrico Fermi 1, 80055 Portici (Napoli), Italy.

Abstract

In this work, we report recent developments on the use of thinned and micro-structured fiber Bragg gratings (FBGs) as in fiber refractometers. Several etched FBG configurations have been proposed for refractive index measurements and for simultaneous temperature referencing, based on Bragg wavelength shift monitoring. Furthermore, an advanced configuration based on structured FBGs has been proposed as a low cost and high resolution refractive index sensor. Here, theoretical analysis, fabrication techniques and spectral characterizations of the proposed optoelectronic devices are presented.

Keywords: Fiber Bragg Gratings, Refractive Index Measurements, Thinned Fiber Bragg Grating.

1 Introduction

Optical sensors are very attractive in chemical and biochemical applications due to some unique characteristics such as immunity to electromagnetic interference and aggressive environments, high sensitivity and fast response. Examples of integrated optical sensors include direct fiber optic reflectometry [1], Mach-Zehnder interferometers, grating couplers, bend loss waveguides or ARROW waveguides [2] and long period gratings [3].

All the proposed techniques, although interesting and able to provide very accurate measurements, suffer several drawbacks such as the complexity in the multiplexing of the sensor probe within a single optical fiber or the cost of reliable read-out units. On the other hand, in the past several years, FBGs sensors have been widely used in many sensing applications including temperature, strain and pressure measurements [4]. The principle of operation of this class of sensors relies on the dependence of the Bragg resonance on effective refractive index and the grating pitch. Since the effective refractive index is not influenced by the external one for standard optical fibers, no sensitivity to surrounding refractive index (SRI) is expected. However, if fiber diameter is reduced along the grating region, the effective refractive index is significantly affected by external index. As consequence, when the SRI changes, shifts in the Bragg wavelength combined with a modulation of the reflected amplitude are expected.

Based on this line of argument, the authors proposed the Thinned FBGs (ThFBGs) as refractive index sensors. HF based chemical etching was used to reduce the cladding layer and a proper package for the sensor fabrication and further characterization and testing was designed [5-7]. Successively, non uniform ThFBGs were proposed as self temperature referenced refractive index sensors [8]. The experimental results, here presented, demonstrated the excellent capability of the proposed devices as advanced fiber refractometers. The read out approach in both cases relies on the detection of the wavelength shift in the Bragg resonance related to the measurand variation. In order to develop low cost tools to be efficiently used in environment monitoring applications, a different approach involving less sophisticated and expensive interrogation units is required. To this aim, a novel configuration based on structured FBGs was proposed. Here the thinning of the cladding layer occurs selectively along the grating region [9]. The perturbation acts as a defect state within the periodic grating structure, leading to significant modifications in the spectral response of the device, including the formation of allowed wavelengths within the grating stop-band [9]. The adopted configuration allows the implementation of low cost read out unit based on the power detection at fixed wavelength [10]. In this paper, a detailed report including the experimental results on the modeling and fabrication of the proposed devices is presented.

2 Uniform ThFBGs as Refractive Index Sensors

As well known, Bragg resonance condition can be expressed as [4]:

$$\lambda_B = 2n_{eff}\Lambda \qquad (1)$$

where, n_{eff} is the effective refractive index of the fiber, Λ is the grating pitch and λ_B is the reflected Bragg wavelength. In common optical fibers, the effective refractive index, $n_{eff,}$ of the fundamental mode is practically independent from the SRI. However, if the cladding diameter is reduced, n_{eff} shows a non linear dependence on SRI, leading to a shift in the reflected wavelength. Differently from common use of this class of sensors for temperature and strain measurements, in this case, only the refractive index n_{eff} is affected by measurand changes while the grating pitch was practically unchanged. In order to outline the dependence of the sensor response on cladding diameter and SRI, n_{eff} in a thinned optical fiber was evaluated by numerically resolving the dispersion equation of a doubly cladding fiber model [7]. Figure 1 shows the non-linear behavior of n_{eff} in a thinned optical fiber versus SRI in the range 1.333-1.455 at an operating wavelength of 1550 nm for different cladding diameters, D_{Th}. Here full etching curve is referred to a completely removed cladding. For the SRI around 1.333, the guided mode is well confined in the core region, leading to a weak dependence on the SRI. As SRI increases, higher sensitivity is observed, since the fundamental mode is less confined in the core region leading to an increased interaction with the external medium. In addition, such interaction and as a consequence sensor sensitivity increases as cladding diameter is reduced under 20µm, reaching its maximum in the case of cladding layer completely removed (full etching).

The fabrication of the thinned FBG sensor can be easily obtained with low cost equipment by wet chemical etching in a buffered hydrofluoric acid (HF) solution [5-7]. In the figure 2.a, a schematic diagram of the experimental setup for sensor preparation is shown. Since the etching step would reduce the diameter of the sensing optical fiber leading to a significant weakening of the overall structure, a proper package is designed and manufactured. A cylindrical test-tube was completely realised in PMMA (poly methyl methacrylate) in order to avoid any chemical interaction between the holder and the HF solution. The fiber was fixed at the two bases using an epoxy based resin (EPON 828 by SHELL) and dual functionalities pipes were arranged along the test tube for washing the realized sensor after HF etching and the injection of liquids for further refractive index measurements.

Before the etching starts, the remaining part of the optical fiber (still covered with coating) was protected by depositing Teflon layers by spray-coating technique. HF aqueous solution at 24% was then added to the test-tube allowing etching rates of the order of 0.65µm/min at 24°C (room temperature). To stop the etching process at the desired depth, the HF solution was removed and the test-tube filled for 15

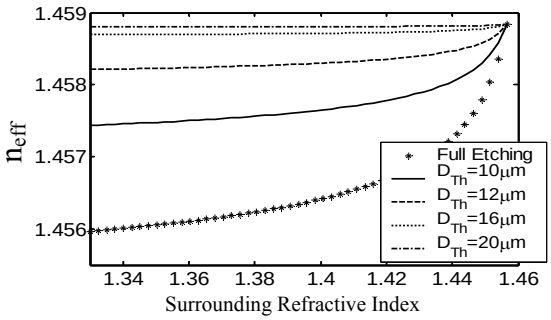

Figure 1: n_{eff} versus SRI for different cladding diameters.

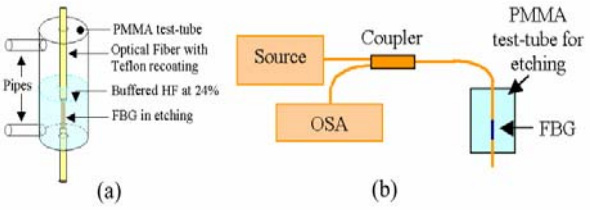

Figure 2: (a) Schematic of the PMMA package; (b) experimental set-up for refractive index measurements.

minutes with a basic solution (calcium oxide). All the fabrication steps were monitored. The optoelectronic set-up, involved for both fabrication process monitoring and for further refractive index measurements, is shown in figure 2.b. It comprises a broadband superluminescent diode (2mW) operating at 1550nm with 40nm FWHM (Full Width Half Maximum), a directional 3dB coupler to collect the reflected spectrum from the sensor head and an optical spectrum analyzer for spectral measurements. Grating spectra measurements have been carried out by recording the reflected spectrum from the sensing grating for each liquid sample. Centroid analysis was used for Bragg wavelength identification allowing resolution in wavelength of the order of 10pm over the whole investigated range. Figure 3.a shows the experimental behavior of the Bragg wavelength during the etching process. For the first 170 minutes, an increasing of λ_B is observed. This effect could be attributed to an increasing in the strain state along the thinned and weak region, due to a not perfect arrangement of the optical fiber. A complete understanding of this aspect is actually under investigation. After 170 minutes, corresponding to a residual cladding diameter of approx. 20µm, a diminution in the n_{eff} and then in the Bragg wavelength is observed. Points (A) and (B) in figure 3.a indicate the end of the etching process and the washing of the sensor head with pure water, respectively. The difference between the Bragg wavelengths in the two different conditions (approx. 1.13nm) is due to the refractive index difference between HF solution and water. In the case of full etched fiber a final shift of 3nm in the Bragg wavelength shift between unperturbed and etched grating with water as external medium was measured.

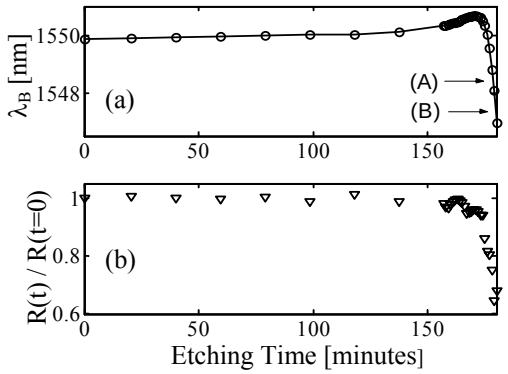

Figure 3: (a) Bragg wavelength and (b) maximum reflectivity percentage variation versus etching time.

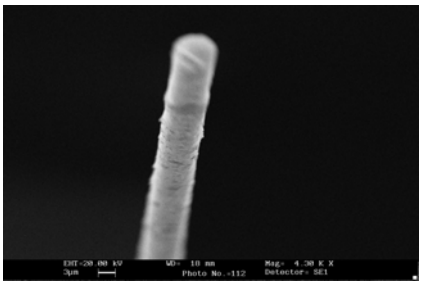

Figure 4: SEM photogram of the thinned optical fiber for the cladding diameter measurement.

During the etching process, combined with a shift in the Bragg wavelength, peak reflectance diminution occurs. Figure 3.b shows the relative peak reflectivity observed during the etching process. At the end of the etching process, the peak reflectivity demonstrated a diminution of about 30% with water as external medium. This effect can be explained by considering the different numerical aperture between the unperturbed fiber and the etched region. The losses induced in the etching process can be lowered by adopting a lower etching depth or surrounding media with higher refractive index.

SEM photogram, reported in figure 4, shows a full etched ThFBG with a diameter of approx. 8μm. In order to test the sensor performance aqueous glycerine solutions at different concentrations were used as external media. A commercial Abbe refractometer with a resolution of 10^{-4} was used for reference characterization. Figure 5 shows the measured wavelength shift referred to the original Bragg wavelength as function of SRI at room temperature (dotted line) together with the numerical one obtained in the case of 8.5μm etched sensor (solid line). This value is very close to the SEM results. From these results and in the case of interrogation units able to discriminate 1pm wavelength shift around 1550nm, refractive index resolutions of $\approx 10^{-5}$ and $\approx 10^{-4}$ are possible for almost full etched sensor and for SRI around 1.45 and 1.333, respectively. In addition, the diminution in the FBG peak reflectivity due to the etching process is not able to influence the

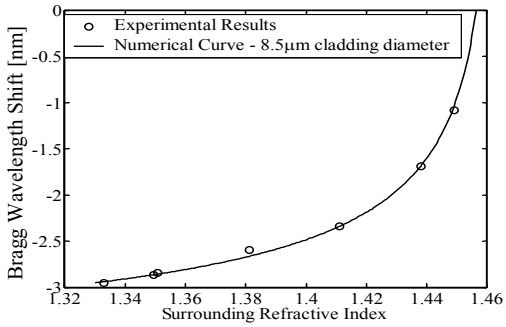

Figure 5: Wavelength shift of the reflected signal of the thinned Bragg filter (dotted line) and the numerical curve (solid line) with cladding diameter of 8.5μm versus external medium.

system performance for most of the interrogation units proposed in literature. Finally, the intrinsic multiplexing capability of FBG based sensors would enable the possibility to implement an all fiber refractive index sensor array by involving wavelength division multiplexing techniques.

3 Non Uniform ThFBGs: Self Temperature Referencing

Based on the results reported here, ThFBGs seem suitable as refractive index sensors and chemical sensors if functionalized overlays are used. However, the compensation of the thermal changes close to the sensing element is necessary when in situ investigations in non controlled environments are required. A first approach is provided by adding a standard grating element sensitive only to thermal changes [11]. This approach, although efficient for single point monitoring, is not the suitable solution when a large number of spatial locations have to be monitored. As valid alternative without using an additional grating element, the use of a single non uniform ThFBG for the simultaneous measurements of refractive index and temperature was proposed by the authors [8].

The structure relies on a standard grating: in part of the sensing element, the cladding layer is partially or totally removed. In these conditions, the etched structure would exhibit a spectral response depending on the local temperature and the surrounding refractive index, while the remaining part would respond only to local thermal changes [8]. The main effect of the perturbation is the splitting of the spectral response of the original grating in two peaks located at two distinct wavelengths in dependence of the etching features and of the external refractive index, according to:

$$\lambda_U = 2 \cdot n_{effU} \Lambda$$
$$\lambda_{Th} = 2 \cdot n_{effTh} \Lambda \qquad (2)$$

where λ_U and λ_{Th} are the Bragg wavelengths and n_{effU} and n_{effTh} are the effective refractive index of the

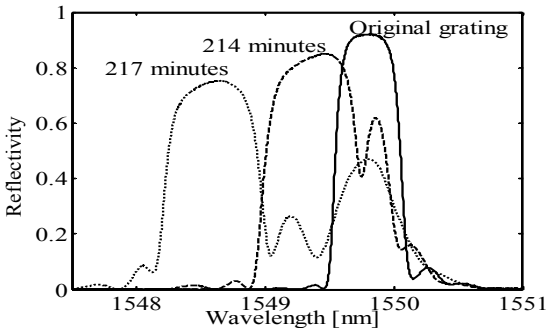

Figure 6: Reflected spectra during the etching process.

unperturbed and thinned grating region, respectively. The sensitivities of the device in terms of wavelength shift are provided in eqs. 3, where α is the thermal expansion coefficient of the fiber, assuming the same value for the two grating regions.

$$\frac{\Delta\lambda_U}{\lambda_U} = \left(\frac{1}{n_{effU}} \frac{\Delta n_{effU}}{\Delta T} + \alpha \right) \Delta T \tag{3.a}$$

$$\frac{\Delta\lambda_{Th}}{\lambda_{Th}} = \left(\frac{1}{n_{effTh}} \frac{\Delta n_{effTh}}{\Delta T} + \alpha \right) \Delta T + \left(\frac{\Delta n_{effTh}}{n_{effTh}} \right)_{\Delta n_{outNT}} \tag{3.b}$$

where the subscript NT represents the SRI change due to chemical agents at a fixed temperature. Obviously, the Bragg wavelength related to the unperturbed region λ_U is sensitive only to local temperature changes according to eq. 3a. Whereas, the Bragg wavelength related to the thinned region λ_{Th} (eq. 3b) would respond to both effects.

It is worth noting that the thermal sensitivity of the thinned region would depend on the thermo-optic coefficient of the surrounding medium, in the case of liquids it is generally negative leading to a slightly lower sensitivity in respect to the unperturbed one.

Also in this case particular care was devoted to packaging and masking. To the aim of decreasing the strain induced on the thinned fiber region, as in previous experimental configuration, a new and more efficient holder, based on a plastic tube and epoxy resin, was realized. In particular, the FBG was arranged in the etching holder positioning with about half of the sensing element inside the plastic tube. Then it was filled up with epoxy resin to protect the fiber. Finally a test tube with dual functionalities pipes is arranged around the holder, for washing the realized sensor after HF etching and the injection of liquids for further refractive index measurements. The new etching holder configuration allowed a good optical fiber arrangement, assuring strain free operation and thus a good degree of reproducibility of the etching process.

Figure 6 shows the spectral responses of the device during the etching process, referred to the original one. According with the theoretical analysis, during the etching process the Bragg reflected signal splits in two lobes. The first one, at the original Bragg

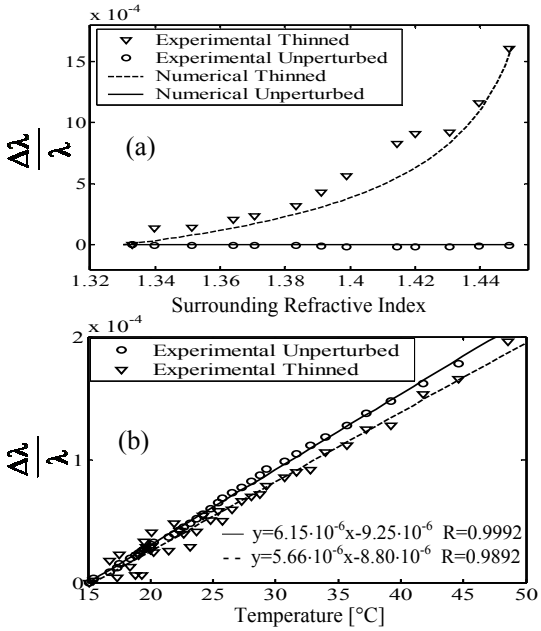

Figure 7: Relative shift for the thinned and the unperturbed wavelengths: (a) versus the external refractive index and (b) versus the temperature.

wavelength, is due to the unperturbed grating region, while the other one corresponding to the etched region moves to lower wavelength. This effect is due to the decrease in the effective refractive index induced by the interaction with the solution with refractive index lower than the cladding one. Figure 7.a shows the relative Bragg wavelength shifts of the two peaks induced by variations in the surrounding refractive index at a temperature of 25°C. As expected, the wavelength corresponding to the etched region exhibits a non linear behaviour with the surrounding refractive index, with increasing sensitivity as SRI approaches the cladding refractive index. Sensitivities of $7.8 \cdot 10^{-2}$ and $3.4 \cdot 10^{-3}$ have been obtained for SRI around 1.45 and 1.33, respectively. On the other side, no changes in the wavelength corresponding to the unperturbed grating region occur. To predict the refractive index sensitivity, numerical analysis has been carried out by using the three layer fiber model and the multilayer approach [5,7]. Good agreement with experimental results was found for a thinned diameter of 7.6μm, very close to the value obtained by the SEM analysis, revealing a residual diameter of approx. 7-8μm. Finally, the thermal characterization has been carried out by using water as surrounding medium with a thermo-optic coefficient of approx. -10^{-4}/°C. Figure 8.b shows the thermal responses of the two peaks in the range 15-48°C. As expected, the thermal sensitivity of the thinned region is slightly lower than the sensitivity measured for the unperturbed region. In addition, in both cases, linear behaviour was found with sensitivities of $6.15 \cdot 10^{-6}$/°C and $5.66 \cdot 10^{-6}$/°C for the unperturbed and thinned regions, respectively. In this case, resolution of 0.1°C can be obtained by using the same detection units with 1pm resolution. Based on

the obtained results, the proposed configuration involving non-uniform ThFBGs demonstrated the potentiality to perform simultaneous and accurate measurements of refractive index and temperature. Performances are comparable with those demonstrated by long period grating based refractometers with the advantage to require low cost interrogation systems. In addition, due to the reduced wavelength shift observed in the case of ThFBG, low complexity approaches are necessary for the development of sensor networks especially when dense multiplexing is required.

4 Structured FBGs: Towards New Interrogation Strategies

In both techniques aforementioned, the change in the measurand is directly related to the wavelength shift of the spectral response of the device. In order to minimize the cost of the read out units, a novel configuration involved micro-structured FBGs was proposed [9-10]. A schematic of the micro-structured FBG is shown in figure 8.a. It consists in a localized stripping of the cladding layer with radial symmetry along the grating structure. The parameters of the structure can be resumed as follows: the etching length L_{Th}, thinned diameter D_{Th}, the unperturbed grating regions lengths on both sides of the perturbation L_1 and L_2 respectively, and the cladding and core fiber diameters D_{clad} and D_{co}, respectively.

The introduction of the defect along the grating leads to strong changes in the reflected spectrum. In particular a band-gap is induced in the stop-band structure of the grating, similarly to the effect observed in Phase-Shift Gratings (PSGs) [12]. Differently from them, micro-structured FBGs exhibit a spectral response dependent on the SRI. The principle of operation relies on the optical beating between the spectra of the unperturbed grating regions modulated by the phase shift induced by the perturbation. The stop-band of the new device increases due to the diminution of the length associated to the two lateral grating regions according to the FBG standard rules. Moreover, the destructive interference of the optical signals reflected from the two lateral gratings leads to the formation of allowed state or defect state inside the band-gap according to the Fabry-Perot effect. The spectral position of the defect state inside the stop-band is related to the phase delay introduced by the perturbed region strongly affected by the perturbation features and the SRI. As SRI changes, a modification of the effective refractive index and thus of the phase delay occurs, leading to a wavelength shift of the defect state. On the other side, as the etching length increases, larger phase shift are induced leading to higher sensitivity of the defect wavelength shift on the SRI. While, as the D_{Th} increases, reduced phase shift is induced in the perturbation region, leading to lower sensitivity to SRI variations. Since the sensing element is only a limited portion of the overall structure, the wavelength shift of the whole spectral response of the device is less relevant than spectral modifications induced by refractive index changes [9-10]. This means that intensity measurements based on narrowband interrogation at fixed wavelength seem to be the suitable demodulation strategy to develop low cost and extremely high sensitivity in fiber chemical sensors.

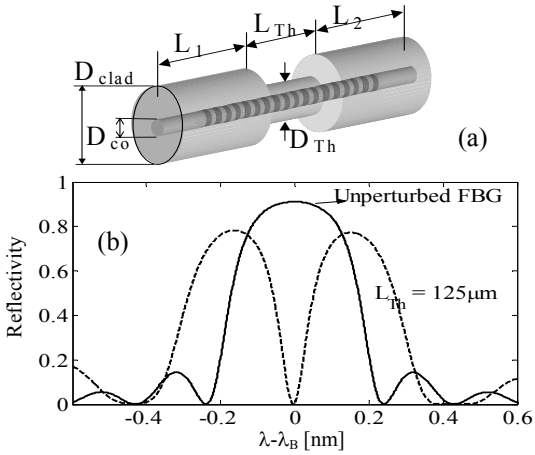

Figure 8: (a) Schematic diagram of the structure (not in scale), (b) spectral response in the case of full etching, L_{Th}=125μm and air as surrounding medium.

Particular attention has to be paid for the fabrication of these devices especially with regard to the masking procedure. Here, a properly protective mask was designed leading to about 700μm long etched region. The holder for the etching is very similar to the package used for the self temperature compensated refractive index probe. In this case, two plastic tubes, arranged on Teflon support, are used to protect the optical fiber on both side of the perturbation. The space between the two tubes corresponds to the etching region, which in turn can be controlled with a resolution of 100μm. The fiber with the grating is arranged inside the tubes, which are filled up with epoxy resin to protect the fiber. Finally a test tube with dual functionalities pipes is arranged on the holder for the etching step. Figure 9.a shows the spectral response of the micro-structured grating with a residual diameter in the etched region of 10.5μm for two different values of SRI, at a fixed temperature of about 20°C. It is worth noting that, differently by the SRI changes, a temperature change induces only a rigid wavelength shift of spectral response of the micro-structured FBG. As observable in figure 9.a, both effects, bandwidth increasing and defect state formation, are evident.

Based on the obtained results a successive experimental step has been carried out by using narrowband interrogation and direct reflectometric interrogation. The optoelectronic setup for refractive index measurements comprises a 3mW laser source tunable in the range 1520-1620nm with a step-resolution of 1pm, a directional 3dB 2x2 coupler to

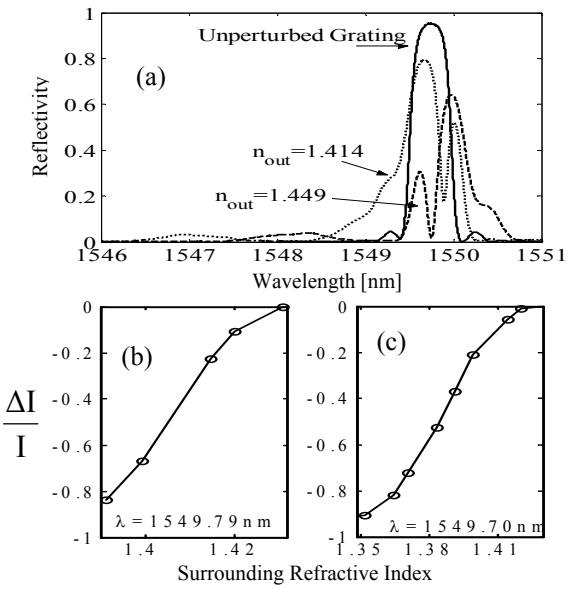

Figure 9: Experimental responses of the micro-structured grating versus the surrounding refractive index in case of L_{etch}=700μm and D_{etch}=10.5μm: (a) Reflected spectrum; (b) Reflectivity at λ=1549.79nm; and (c) Reflectivity at λ=1549.70nm.

collect the reflected signal from the sensor head and to provide an additional channel for power monitoring. Figure 9.b and c show the relative change in the normalized output signals obtained by the ratio between the reflected signals from the structure and the signal devoted to power monitoring for two operating wavelengths 1549.79nm and 1549.70nm, respectively. In the investigated refractive index ranges 1.391-1.420 and 1.364-1.40, the normalized signals change of about 75% and 60%, respectively, leading to refractive index resolutions of $4 \cdot 10^{-5}$ and $6 \cdot 10^{-5}$ by using detection units able to resolve 0.1% intensity changes. It's worth to note that the proposed configuration has been realized with low cost fabrication stages, and exhibits performances in terms of resolution adequate to be used in practical application of environment monitoring.

5 Conclusions

In conclusions, in this work, the activities devoted to the development of reliable and high sensitivity all fiber refractometers to be used in water and environment monitoring applications have been reported. The attention has been focused to develop novel configuration involving uniform, non uniform and selective etching of the cladding layer of FBGs elements. The experimental results confirmed the good performances predicted by the theoretical and numerical analysis. In addition, all the proposed devices involve cost effective equipment for both fabrication and interrogation stages. Main drawback of the presented structures is directly related to the weakening of the sensing probe due to the etching. This aspect could easily addressed by adopting a proper package design, also a microfluidic arrangement could be efficiently used. Future works will address the possibility to design opto-chemical devices by the suitable integration with sensitive and functionalized overlays.

6 References

[1] Cusano A., Cutolo A., Giordano M., Nicolais L., "Optoelectronic Refractive Index Measurements: Applications to Smart Polymer *Processing", IEEE Sensors Journal*, Vol. 3, No. 6, Dec 2003.

[2] Bernini R., Camponiano S., Zeni L., "Silicon Micromachined Hollow Optical Waveguides for Sensing Applications", *IEEE Jour. Selected Topics in Quantum Electron.* Vol. 8, No. 1, 2002.

[3] Falciai R., Mignani A.G., Vannini A., "Long period gratings as solution concentration sensors", *Sensors Actuators B*, 74, 74–77, 2001.

[4] Kersey A.D., Davis M.A., Patrick H.J., LeBlac M., Koo K.P., Askins C.G., Putnam M.A., Friebele E.J., "Fiber Grating Sensors", *Journal Lightwave Technology*, Vol. 15, No. 8, 1442-1463, 1997.

[5] Iadicicco A., Cusano A., Persiano G.V., Cutolo A., Bernini R., Giordano M., "Refractive Index Measurements by Fiber Bragg Grating Sensor", Sensors, *Proceed. IEEE*, Vol. 1, pp. 101-105, Oct.22-24, 2003.

[6] Iadicicco A., Cusano A., Cutolo A., Bernini R., Giordano M., "Thinned Fiber Bragg Gratings as High Sensitivity Refractive Index Sensor", *IEEE Photonics Technology Letters*, Vol. 16, No. 4, 1149-1151, April 2004.

[7] Iadicicco A., Cusano A., Campopiano S., Cutolo A., Giordano M., "Thinned Fiber Bragg Gratings as Refractive Index Sensors", *IEEE Sensors Journal,* Vol. 5, No. 6, December 2005.

[8] Iadicicco A., Campopiano S., Cutolo A., Giordano M., Cusano A., "Non-Uniform Thinned Fiber Bragg Gratings for Simultaneous Refractive Index and Temperature Measurements", *IEEE Photonics Technology Letters*, Vol. 17, No. 7, July 2005.

[9] Iadicicco A., Campopiano S., Cutolo A., Giordano M., Cusano A., "Micro-Structured Fiber Bragg Gratings: Analysis and Fabrication", *IEE Electronic Letters*, Issue 8, 466, April 2005.

[10] Iadicicco A., Campopiano S., Cutolo A., Giordano M., Cusano A., "Refractive Index Sensor Based on Micro-Structured Fiber Bragg Grating", *IEEE Photonics Technology Letters* Vol. 17, No. 6, June 2005.

[11] Pereira D.A., Frazao O., Santos J.L., "Fiber Bragg grating sensing system for simultaneous measurement of salinity and temperature", *Optical Engineering*, Vol. 43, pp. 299, 2-2004.

[12] Wei L., Lit J.W.Y., "Phase Shifted Bragg Grating Filters with Symmetrical Structures", *Jour. Lightwave Technology.*, Vol. 15, 1997.